Available online at www.sciencedirect.com
ScienceDirect
Journal of Power Sources 165 (2007) 420–426
JOURNAL OF POWER SOURCES
www.elsevier.com/locate/jpowsour

A hybrid power source with a shared electrode of polyaniline doped with $LiPF_6$

Kwang Sun Ryu *, Kwang Man Kim **

Ionics Devices Team, IT-NT Group, IT Convergence & Components Lab., Electronics & Telecommunications Research Institute (ETRI), 161 Gajong, Yusong, Daejon 305–700, South Korea

Received 10 October 2006; received in revised form 21 November 2006; accepted 21 November 2006
Available online 12 January 2007

Abstract

We fabricated a hybrid power source device with three electrodes of which one was a $LiPF_6$-doped polyaniline (PAn) electrode playing the roles of both the positive electrode of a lithium secondary battery and an electrode of a redox supercapacitor. As a consequence, the shared electrode acts as a positive electrode or a positive terminal of a hybrid power source. The negative terminal was connected between a lithium metal electrode and another $LiPF_6$-doped PAn electrode. After characterizing and comparing this hybrid power source with a single lithium secondary battery, its discharge performance was superior to that of a single lithium secondary battery when adopting the sheet-type PAn-$LiPF_6$ electrodes and the porous separator as an electrolyte medium. In this case, the hybrid power source was shown to be advantageous in the high pulse mode of discharge.

Keywords: Hybrid power source; Lithium secondary battery; Redox supercapacitor; Polyaniline electrode; $LiPF_6$ doping

1. Introduction

We currently live in a highly developed information-oriented society where individual and commercial information is highly valued. Consequently, reliable information communication systems are required such as mobile cellular phones, laptop computers, and more developed portable terminals of digital multimedia broadcasting (DMB) and wireless broadband Internet (WiBro). Benign electrical energy sources are inevitably needed for operating these information communication systems. Moreover, there is a requirement that an excellent energy storage system should be used in more effective information communication systems. In this respect, much interest has been concentrated on lithium secondary batteries and redox supercapacitors as energy sources. In lithium secondary batteries and other related rechargeable power sources, cell potential and energy density strongly depend on the positive electrode material. For practical use and commercial production of lithium secondary batteries and redox supercapacitors, high-quality positive electrode materials must be developed, or the characteristics of existing positive electrode materials must be greatly improved, to approach their theoretical capacities.

Layered, three-dimensional compounds are presently used primarily as positive electrode materials for lithium secondary batteries [1]. Many attempts to use polymer materials such as organic sulfide [2] and conducting polymer [3] as positive electrode materials have been made, and some studies utilizing inorganic or organic hybrid electrodes are underway [4]. Of these, electrically conducting polymers such as polyaniline (PAn), polypyrrole, and polythiophene are expected to be very promising electrode materials for lithium secondary batteries and redox supercapacitors because they have good electrochemical properties along with air-stability [5].

On the other hand, lithium secondary batteries are, in general, not easy to charge/discharge at a high rate, whereas redox supercapacitors can operate at a high rate of charge/discharge but cannot supply power for prolonged times [6]. In this regard, there have been many studies focused on the development of a power source capable of charging/discharging at both high and low rates by hybridizing the battery and capacitor components. Consequently, many kinds of hybrid power sources have been developed by some combination among secondary batteries, supercapacitors, fuel cells, and even solar cells [7–10]

* Corresponding author. Tel.: +82 42 860 5517; fax: +82 42 860 6836.
** Corresponding author. Tel.: +82 42 860 6829; fax: +82 42 860 6836.
E-mail addresses: ryuks@etri.re.kr (K.S. Ryu), kwang@etri.re.kr (K.M. Kim).

0378-7753/$ – see front matter © 2006 Elsevier B.V. All rights reserved.
doi:10.1016/j.jpowsour.2006.11.066

with series and/or parallel connections. In this paper, we suggest a new concept of a hybrid power source having one shared electrode with the redox reaction occurring. Our system is composed of three electrodes including a lithium metal electrode and two lithium-doped polyaniline (PAn-Li) electrodes, concurrently providing dual functions of a lithium secondary battery and a redox supercapacitor. Charge/discharge characteristics of this hybrid power source were investigated and compared with that of a single lithium secondary battery.

2. Experimental

Fig. 1(a) shows the schematic view of the newly developed hybrid power source including the units of a lithium secondary battery and a redox supercapacitor in the cell with a shared electrode of PAn-Li. This hybrid power source has three electrodes, one lithium metal and two PAn-Li electrodes with the same electrolyte. Each electrode is separated by a porous polyethylene separator or, in some cases, by a polymer electrolyte. The lithium secondary battery works by combining lithium metal (A) as a negative electrode and the PAn-Li (B) as a positive electrode. The redox supercapacitor operates by combining two PAn-Li electrodes of (B and C). The PAn-Li (B), which functions as the positive electrode of the lithium secondary battery and the one electrode of the redox supercapacitor, is a shared electrode of the positive terminal of the hybrid power source. The lithium metal material (A), acting as the negative electrode of the lithium secondary battery, and the PAn-Li (C), acting as the other electrode of the redox supercapacitor, are connected with the negative terminal of the hybrid power source.

The synthesis details of the PAn powder from emeraldine base can be found in a previous report [11]. The doping of lithium hexafluorophosphate ($LiPF_6$) as a lithium salt to make the PAn-$LiPF_6$ powder sample is also described in detail elsewhere [12,13]. An electrolyte solution (Mitsubishi Chemicals) of 1 M $LiPF_6$ dissolved in an equal volume mixture of ethylene carbonate (EC) and dimethyl carbonate (DMC) was used in this doping process. The term "PAn-Li electrode" above denotes the PAn-$LiPF_6$ electrode throughout the present work. Two types of PAn-Li electrode were then prepared: lump-type and sheet-type electrodes by dry and wet processes, respectively. The powdered PAn-$LiPF_6$ lump was obtained in a mortar apparatus by mixing the PAn-$LiPF_6$ powder, carbon black (Super P, MMM Carbon) as a conductive agent, and poly(tetrafluoroethylene) powder (Aldrich) as a polymer binder with a weight ratio of 2:2:1. The powdered-lump was placed on aluminum foil (15 μm thick) to function as a current collector and compressed with pressure to give the lump-type PAn-Li electrode. It should be noted that the shared electrode (B) in Fig. 1(a) had the PAn-Li electrodes on both sides of the aluminum foil current collector while the other electrode (C) was on one side of aluminum foil.

The sheet-type PAn-Li electrode was prepared by the following steps. The PAn-$LiPF_6$ powder, carbon black (Super P, MMM Carbon), poly(vinylidene fluoride-co-hexafluoropropylene) (PVdF-HFP) (KynarFlex 2801, Atofina Chemicals) as a polymer binder, and acetone as a solvent were mixed for 72 h at room temperature by a magnetic bar in a sealed bottle to make a viscous slurry. The weight ratio of PAn-$LiPF_6$:Super P:KynarFlex 2801 was fixed at 42:28:30. The slurry was cast on a polyethylene film using a doctor blade apparatus and dried in a vacuum oven at 50 °C for 12 h. The PAn-$LiPF_6$ film formed on the polyethylene film was peeled off and then laminated on both sides of an aluminum mesh or expanded metal (30 μm thick, Exmet Co.) to use as the shared PAn-Li electrode (B) in Fig. 1(a). The total thickness and the active mass of this PAn-$LiPF_6$ electrode were ~115 μm and 1.580 mg cm^{-2}, respectively. The other PAn-Li electrode (C) in this case was obtained by attaching the PAn-$LiPF_6$ film on one side of aluminum foil (15 μm thick).

In order to fabricate the hybrid power source device using the lithium metal (A) and the PAn-Li electrodes (B and C), each with a size of 2 cm × 2 cm, a pouch cell was prepared as shown in Fig. 1(b), which was composed of (A)||E||(B)||E||(C) with the electrical connection between (A and C). Here, the E denotes a sheet of porous separator of polypropylene (PP)/polyethylene (PE)/PP film (Celgard) or a polymer electrolyte sheet [14] consisting of 90 wt% PVdF-HFP and 10 wt% fumed silica (SiO_2) after absorbing the electrolyte solution. The constituents in Fig. 1(b) were then sandwiched in sequence by a laminating method with a double-roll press under a line pressure of 40 kgf cm^{-1} at 120 °C. Before sealing the cell with an Al-pouch, the electrolyte solution of 1 M of $LiPF_6$ dissolved in the mixture

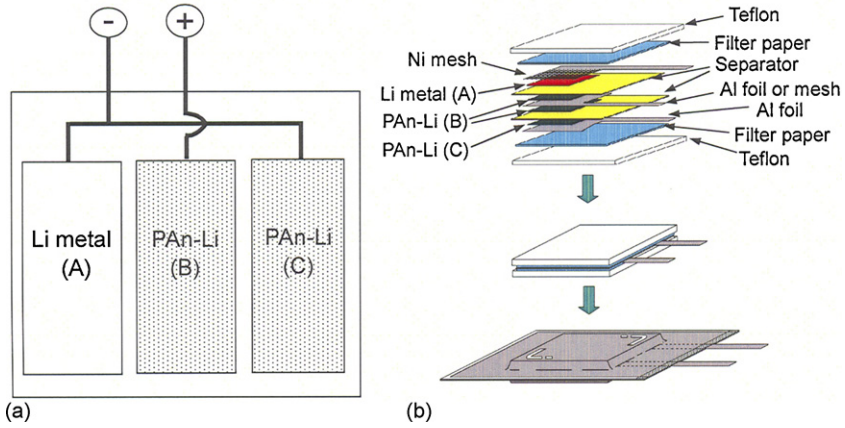

Fig. 1. (a) Schematic view and (b) fabrication steps of the hybrid power source cell with a shared electrode.

of EC and DMC (1:1, v/v) was injected to sufficiently wet the cell constituents. For comparison, a single lithium secondary battery consisting of (A)||E||(B) (i.e., Li||E||PAn-LiPF$_6$) was also prepared. All these fabrication steps were performed in a dry room with the moisture content less than 0.1 ppm. A single redox supercapacitor consisting of (B)||E||(C) was also prepared by using just two PAn-Li electrodes to examine its electrical capacitance under repeated charge/discharge cycling.

As a preliminary test of the hybrid power source, the single lithium secondary battery using the Li and sheet-type PAn-Li electrodes was repeatedly charged/discharged over 100 times by using a galvanostatic cycler (Maccor Co.) in the voltage range of 2.8–4.2 V. In this test, the charge current was set to 0.025 mA cm^{-2} while setting the discharge current to 0.125 mA cm^{-2}. A single redox supercapacitor using two sheet-type PAn-Li electrodes was also tested in the same manner in the range of 0.01–1.0 V with the applied current densities of 0.025 mA cm^{-2} at charging and 2.5 mA cm^{-2} at discharging. As main tests for the hybrid power source cell of (A)||E||(B)||E||(C), three kinds of cells were prepared and repeatedly cycled with various pulsed discharge modes. The different hybrid power source cells were composed of: (i) lump-type (B and C) electrodes divided by porous separator films (Celgard), (ii) sheet-type (B and C) electrodes divided by porous separator films (Celgard), and (iii) sheet-type (B and C) electrodes divided by the polymer electrolyte sheet [14] consisting of 90 wt% PVdF-HFP and 10 wt% fumed silica (SiO_2). The same conditions of constant-current charge (up to 4.0 V) and the subsequent pulse-mode discharge (down to 2.5 V) were applied to each hybrid power source cell. A constant-current discharge at low current for 10 min followed by another constant current at high current discharge for 10 s was repeated during the discharge process. The high current used was 20–50 times greater than the low current. In addition, all discharge patterns of the hybrid power source cells were compared with those of the single lithium secondary battery obtained under the same charge/discharge conditions.

3. Results and discussion

3.1. Charge/discharge mechanisms

In Fig. 2, the two combinations of (A)||E||(B) and (B)||E||(C) comprise the lithium secondary battery and redox supercapacitor, respectively. It is thus noteworthy that the shared electrode (B) simultaneously plays both roles of a cathode of the lithium secondary battery and an electrode of the redox supercapacitor. The charge separation mechanism in the Li||PAn-LiBF$_4$ [15] or Li||PAn-LiPF$_6$ battery [16] as shown in Fig. 2(a) may be very useful in describing the charge process of the present

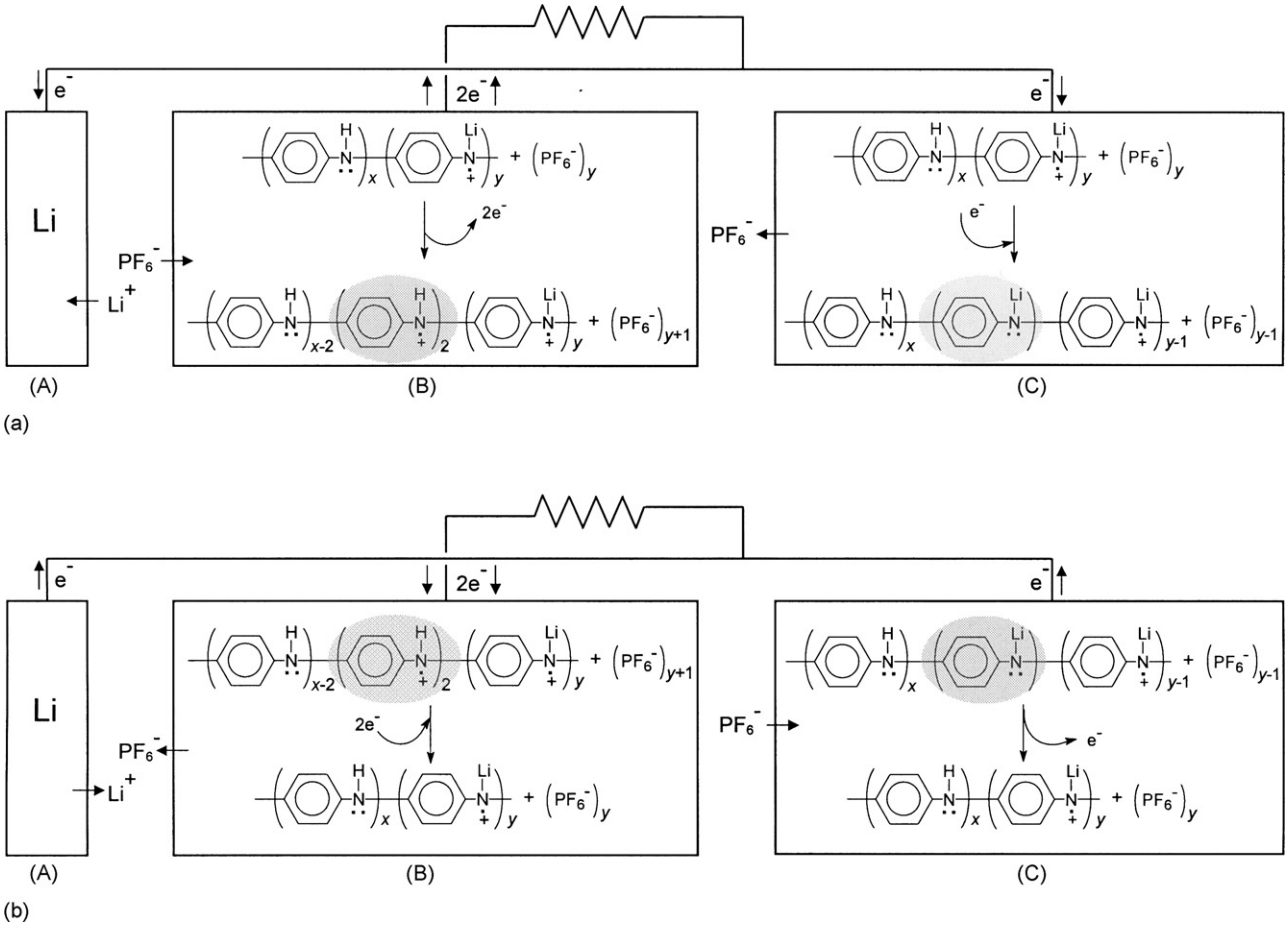

Fig. 2. Prospective reactions during: (a) charge and (b) discharge in the present hybrid power source model.

hybrid power source. In the charge process, it is expected that two unpaired electrons are generated in amide nitrogen in the shaded region of the electrode (B), which is very similar to the charge separation mechanism [16]. Then, one electron moves to the lithium electrode (A) to transform Li^+ into metallic Li^0 while the other electron goes to the electrode (C) to give another benzenoid structure in a doped state with Li^+ (i.e., shaded region in the electrode (C) in Fig. 2). Thus, the charging reactions occurred in each electrode are summarized as follows:

(Anode A + C)

$$Li^+ + (An)_x(An\text{-}Li^+)_y(PF_6^-)_y + 2e^- \rightarrow Li^0 + (An)_x(An\text{-}Li)(An\text{-}Li^+)_{y-1}(PF_6^-)_{y-1} + PF_6^- \quad (1)$$

(Cathode B)

$$(An)_x(An\text{-}Li^+)_y(PF_6^-)_y + PF_6^- \rightarrow (An)_{x-2}(An^+)_2(An\text{-}Li^+)_y(PF_6^-)_{y+1} + 2e^-. \quad (2)$$

It is noteworthy that a possibility of another product in the electrode (B), such as $(An)_x(An\text{-}Li)_2(An\text{-}Li^+)_{y-2}(PF_6^-)_{y+1}$, can be excluded by the charge separation mechanism in PAn-$LiPF_6$ system [16]. Thus, the overall charging reaction becomes

$$Li^+ + 2(An)_x(An\text{-}Li^+)_y(PF_6^-)_y \rightarrow Li^0 + (An)_x(An\text{-}Li)(An\text{-}Li^+)_{y-1}(PF_6^-)_{y-1} + (An)_{x-2}(An^+)_2(An\text{-}Li^+)_y(PF_6^-)_{y+1}. \quad (3)$$

The discharge reaction can occur in the opposite direction of charge reaction mechanism. In the aspect of the electrolyte medium, the dissociated ions such as Li^+ and PF_6^- have their ionic tendency to migrate to each electrode with respect to charge/discharge processes. That is, PF_6^- anions migrate to the shared electrode (B) to balance with the oxidated state of PAn in the charge process. Meanwhile, Li^+ cations move in the opposite direction to be deposited as metallic Li^0 on the lithium electrode (A) or to balance with the reduced state of PAn on the electrode (C). In the discharge process, Li^+ cations and PF_6^- anions escape from the electrodes (A) and the shared electrode (B), respectively. As a remark, the use of $LiPF_6$ rather than lithium tetrafluoroborate ($LiBF_4$) as a lithium salt is based upon the fact that the electrolyte solution containing $LiPF_6$ exhibits a higher specific discharge capacity in the PAn-$LiPF_6$ electrode than the PAn-$LiBF_4$ system [17,18]. In addition, it should be noted that the concentration of $Li^+PF_6^-$ salt may be an important factor to control the degree of the charge separation mechanism [15,16].

3.2. Performances of battery and capacitor

Fig. 3 shows the cycle performances of the single lithium secondary battery and the single redox supercapacitor which were fabricated individually using the sheet-type PAn-Li electrodes and different types of electrolytes (i.e., PP/PE/PP separator or PVdF-HFP polymer electrolyte). As shown in Fig. 3(a), the specific discharge capacity of the single lithium secondary battery increased initially and then saturated over repeated cycles.

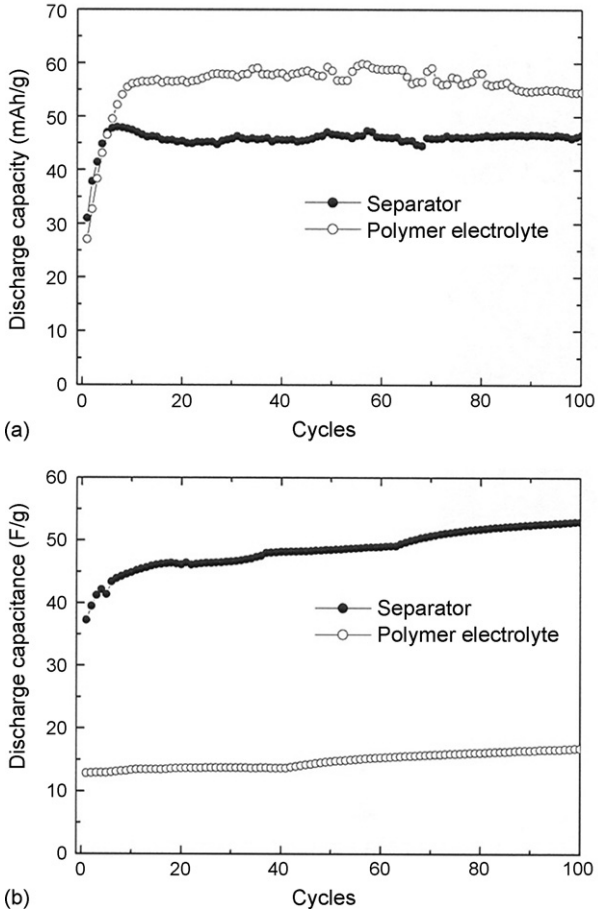

Fig. 3. (a) Discharge capacities of a single lithium secondary battery of (A)||E||sheet-type (B) (i.e., Li||E||PAn-Li) and (b) discharge capacitances of single redox supercapacitors of sheet-type (B)||E||sheet-type (C) (i.e., PAn-Li||E||PAn-Li). A porous separator, E, of PP/PE/PP film (Celgard) or a polymer electrolyte sheet [14] was used after absorbing the 1 M $LiPF_6$/EC:DMC (1:1, v/v) electrolyte solution.

This is probably due to the gradual increase and the subsequent saturation of active sites or reaction paths during the repeated charge/discharge cycles. This is consistent with previous results when a glass filter was used instead of a separator [17]. However, the battery utilizing the PVdF-HFP polymer electrolyte shows a higher saturated discharge capacity of ~56 mAh g^{-1} than that of the battery using a PP/PE/PP separator (~47 mAh g^{-1}). Also, referring to the discharge capacity (~50 mAh g^{-1}) of the battery using a glass filter [17], the difference in the saturated discharge capacity may be due to the difference in the absorption degree or the uptake of electrolyte solution among the separating mediums (i.e., higher capacity is observed in the order of the batteries using PVdF-HFP polymer electrolyte, glass filter, and PP/PE/PP separator). It should be noted here that the highest discharge capacity is only about 40% of the theoretical capacity of the PAn-Li electrode (142.6 mAh g^{-1}). Thus, there seems to be opportunities for further increases in the capacity by some modifications of electrode and/or electrolyte systems. For instance, the use of a nucleophilic dopant such as dimethyl sulfate in the PAn electrode, instead of lithium salt, may increase the saturated discharge capacity [19]. It is also noteworthy that

the polymer electrolyte is more advantageous in the discharge capacity because it enables the higher discharge rate (just five times the charge rate) compared to the PP/PE/PP separator.

On the other hand, Fig. 3(b) shows the discharge capacitance of the single redox supercapacitor (B)||E||(C) with different electrolyte media obtained with a discharge rate 100 times higher than the charge rate. Though the discharge capacitances in the figure are somewhat lower than the previous results [12,13] obtained using 1 M Et_4NBF_4 salt in acetonitrile as an electrolyte solution, the present case uses 1 M $LiPF_6$ in EC/DMC to satisfy the requirements of both the lithium secondary battery and the supercapacitor. Contrary to the case of the lithium secondary battery in Fig. 3(a), the redox supercapacitor exhibits higher capacitance (~50 F g^{-1} at 50th cycle) in the case of using PP/PE/PP separator than that of polymer electrolyte (~15 F g^{-1} at 50th cycle). This may be due to the rapid electrochemical reaction occurring on the electrode surface which is regarded as a typical characteristic of capacitors. That is, the porous separator is more advantageous in the discharge capacitance than the polymer electrolyte because the retention of electrolyte solution in the electrolyte medium does not affect the characteristics of the redox supercapacitor. This is probably why the discharge capacitance of redox supercapacitor is mainly raised by the surface reaction between (B)||E||(C), not by the amount of liquid electrolyte absorbed and preserved within the polymer electrolyte. The advantage of separator is also true in the case of using Et_4NBF_4 salt in acetonitrile [12].

3.3. Discharge patterns of hybrid power source cells

When this hybrid cell is charged and/or discharged, the lithium metal material (A) and the shared electrode (B) become a negative electrode and a positive electrode, respectively, in the lithium secondary battery. Also, the shared electrode (B) and the same electrode (C) become two electrodes of the redox supercapacitor. As a main concept of the present hybrid power source cell, the redox supercapacitor part (B)||E||(C) is discharged for a short time at a high rate whereas the lithium secondary battery part (A)||E||(B) is usually discharged at a low rate to supply energy for a somewhat longer time. Due to the different discharge modes, the hybrid cell can be expected to exhibit more rapid energy conversion than the lithium secondary battery and, concurrently, to work as an energy reservoir for a longer time than the redox supercapacitor.

Fig. 4 shows the discharge performances of a hybrid power source cell and a lithium secondary battery where both utilized the lump-type PAn-Li electrodes and the PP/PE/PP separator. Fig. 4(a and b) are the discharge curves at the 20th and 50th cycles, respectively, under the constant-current charge of 0.0625 mA cm^{-2} for 10 min and the subsequent pulsed discharge at a rate 40 times higher than the constant current for 10 s. Meanwhile, Fig. 4(c and d) are the similar cases in which the applied currents were nearly doubled. At a low charge rate and the subsequent discharge at 0.0625 mA cm^{-2}, as shown in Fig. 4(a and b), the discharge voltage of the hybrid cell is preserved higher than that of lithium secondary battery, and the voltage difference between them is reduced with an increase in discharge time and cycle number. Moreover, the voltage drop of the hybrid cell in the mode of pulsed discharge for 10 s is smaller than that of the lithium secondary battery. These results may be due to the higher capacitive property for the hybrid cell than the single lithium secondary battery. At a high charge rate and the subsequent discharge at 0.125 mA cm^{-2} as shown in Fig. 4(c and d), the voltage drop of hybrid cell is still smaller than that of the

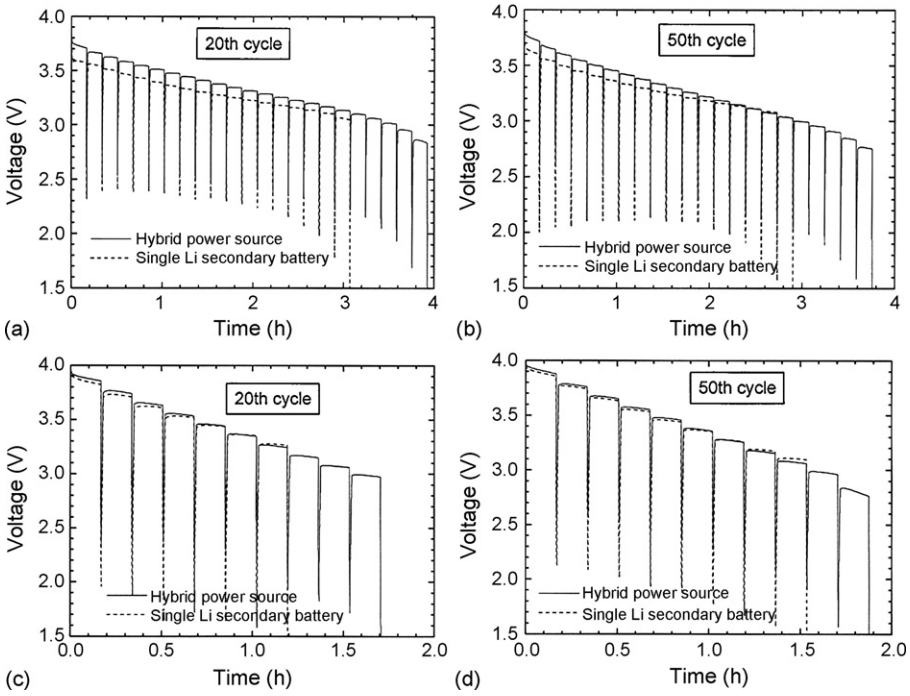

Fig. 4. (a–d) Discharge curves of a hybrid power source and a single lithium secondary battery which are using the lump-type PAn-Li electrode and the porous PP/PE/PP separator and operating between 2.5 and 4.0 V.

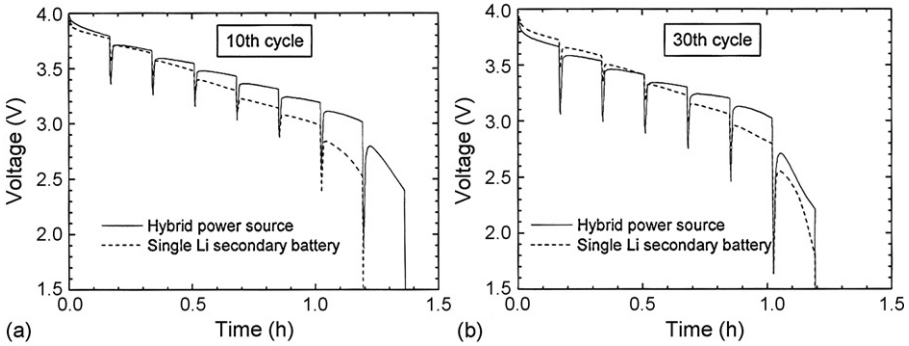

Fig. 5. Discharge curves of a hybrid power source and a single lithium secondary battery which are using the sheet-type PAn-Li electrode and the porous PP/PE/PP separator and operating between 2.5 and 4.0 V.

lithium secondary battery, and also, a steep decrease in the voltage profile, compared to the case of low-rate charge/discharge, is observed. However, the fact that the profile of the discharge voltage with time is nearly consistent between the different cases is unexpected. If this abnormal phenomenon is not an accident, we believe that it is probably due to the rapid reaction occurring on the lump-type PAn-Li electrode of the lithium secondary battery. The lump-type PAn-Li electrode is highly conductive because it embeds more active sites between closely connected particles contrary to the sheet-type PAn-electrode with higher binder content.

The discharge capacities of the hybrid power source cell and the lithium secondary battery utilizing the sheet-type PAn-Li electrodes and the PP/PE/PP separator shown in Fig. 5 were obtained under mild conditions of 0.025 mA cm^{-2} during charging and the subsequent discharge at 0.125 mA cm^{-2}. Here, the pulsed discharge current density is set to 2.5 mA cm^{-2} for 10 s with the interval of 10 min. The discharge voltage of the hybrid cell with an increase in time is higher than that of the lithium secondary battery, and the deviation between them seems to disappear with the cycle number. However, the voltage drops at the pulsed mode of discharge are nearly the same for the hybrid cell and the lithium secondary battery. Contrary to the above results, the case of using the sheet-type PAn-Li electrodes and the PVdF-HFP polymer electrolyte shows discharge capacities with nearly equal voltage profiles for both the hybrid cell and lithium secondary battery as shown in Fig. 6, obtained under the same conditions of charge/discharge and pulsed discharge. The voltage drops at the pulsed mode are also almost equal for them. From these facts, the use of a porous separator in the hybrid cell is advantageous for the preservation of high-voltage discharge capacity because the capacitive property of the cell can be modified if the separator is adopted as in previous redox supercapacitor results [12]. Meanwhile, the hybrid cell using the polymer electrolyte is rather effective in energy storage and/or conversion at a low current rate and, thus, it results in nearly equal discharge curves, as shown in Fig. 6.

4. Conclusion

We report a new hybrid power source composed of three electrodes (a lithium metal, a PAn-$LiPF_6$ shared electrode, and another PAn-$LiPF_6$ electrode), which concurrently play the roles of a lithium secondary battery and a redox supercapacitor. In the hybrid cell, the negative terminal is connected with the negative electrode of the lithium secondary battery to supply small amounts of energy (at a low rate) or connected with the one electrode of the supercapacitor to supply large amounts of energy (at a high rate). In the case of using the powdered-lump as electrode and the porous separator, the hybrid cell had a longer discharge time and more reduced voltage drop than a lithium secondary battery on a pulsed discharging mode. The voltage of the hybrid cell was also higher than that of the lithium secondary battery. This trend coincides with a hybrid cell and lithium secondary battery using the sheet-type PAn-$LiPF_6$ electrode and the porous PP/PE/PP separator. Thus, the present hybrid power

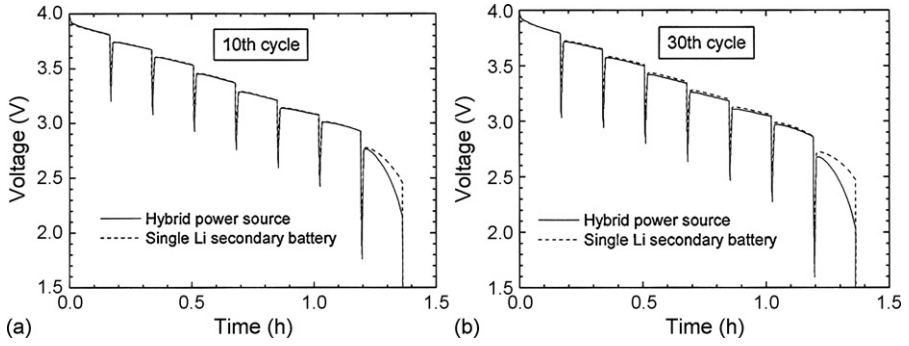

Fig. 6. Discharge curves of a hybrid power source and a single lithium secondary battery which are using the sheet-type PAn-Li electrode and the polymer electrolyte [14] and operating between 2.5 and 4.0 V.

source cell has an advantage in high pulse mode, which can be adapted to a power source for use in electro-vehicle or mobile telecommunication applications.

References

[1] M. Winter, J.O. Besenhard, M.E. Spahr, P. Novak, Adv. Mater. 10 (1998) 725.
[2] N. Oyama, T. Tatsuma, T. Sato, T. Sotomura, Nature 373 (1995) 598.
[3] P. Novak, K. Muller, K.S. Santhanam, O. Haas, Chem. Rev. 97 (1997) 207.
[4] P. Gomez-Romero, Adv. Mater. 13 (2001) 163.
[5] C. Arbizzani, M. Mastragostino, B. Scrosati, in: H.S. Nalwa (Ed.), Handbook of Organic Conductive Molecules and Polymers, John Wiley & Sons, 1997 (Chapter 11).
[6] B.E. Conway, Electrochemical Supercapacitors, Plenum Publishing, New York, 1999.
[7] G.G. Amatucci, US Patent 6,252,762 B1 (2001).
[8] R.A. Huggins, J. Power Sources 134 (2000) 179.
[9] G. Gutmann, J. Power Sources 84 (1999) 275.
[10] G. More, US Patent 6,046,402 (2000).
[11] K.S. Ryu, S.H. Chang, S.G. Kang, E.J. Oh, C.H. Yo, Bull. Korean Chem. Soc. 20 (1999) 333.
[12] K.S. Ryu, K.M. Kim, Y.J. Park, N.-G. Park, M.G. Kang, S.H. Chang, Solid State Ionics 152–153 (2002) 861.
[13] K.S. Ryu, K.M. Kim, N.-G. Park, Y.J. Park, S.H. Chang, J. Power Sources 103 (2002) 305.
[14] K.M. Kim, K.S. Ryu, S.-G. Kang, S.H. Chang, I.J. Chung, Macromol. Chem. Phys. 202 (2001) 866.
[15] K.S. Ryu, K.M. Kim, S.-G. Kang, G.J. Lee, S.H. Chang, Solid State Ionics 135 (2000) 229.
[16] K.S. Ryu, J.H. Jung, J. Joo, S.H. Chang, J. Electrochem. Soc. 149 (2002) A478.
[17] K.S. Ryu, K.M. Kim, S.-G. Kang, J. Joo, S.H. Chang, J. Power Sources 88 (2000) 197.
[18] J.H. Jung, B.H. Kim, B.W. Moon, J. Joo, S.H. Chang, K.S. Ryu, Phys. Rev. B 64 (2001) 035101.
[19] K.S. Ryu, Y.-S. Hong, Y.J. Park, X. Wu, K.M. Kim, Y.-G. Lee, S.H. Chang, S.J. Lee, Solid State Ionics 175 (2004) 759.